Recellularization of auricular cartilage via elastase-generated channels

J. Lehmann[1,2], S. Nürnberger[3,4,9], R. Narcisi[5], K. S. Stok[6,7], B. C. J. van der Eerden[8], W.J.L.M. Koevoet[1], N. Kops[5], D. ten Berge[2*], G.J. van Osch[1,5*^]

[1]Department of Otorhinolaryngology and Head and Neck Surgery Erasmus MC, Rotterdam, the Netherlands

[2]Department of Cell Biology Erasmus MC, Rotterdam, the Netherlands

[3]Ludwig Boltzmann Institute for Experimental and Clinical Traumatology, Vienna, Austria.

[4]Austrian Cluster for Tissue Regeneration, Vienna, Austria

[5]Department of Orthopaedics, Erasmus MC, Rotterdam, the Netherlands

[6]Institute for Biomechanics, ETH Zurich, Zurich, Switzerland

[7]Department of Biomedical Engineering, The University of Melbourne, Parkville, Victoria, Australia

[8]Department of Internal Medicine Erasmus MC, Rotterdam, the Netherlands

[9]Department of Orthopaedics and Trauma-Surgery, Division of Trauma-Surgery Medical University, Vienna, Austria

*these authors contributed equally;

^corresponding author g.vanosch@erasmusmc.nl (Wytemaweg 80, 3000 CA Rotterdam)

Keywords

cartilage tissue engineering, elastin, recellularization, auricular, osteochondral defect

Abbreviated Title

Recellularization of Cartilage via Elastin Fibre Channels

Abstract

Decellularized tissue matrices are promising substrates for tissue generation by stem cells to replace poorly regenerating tissues such as cartilage. However, the dense matrix of decellularized cartilage impedes colonisation by stem cells. Here, we show that digestion of elastin fibre bundles traversing auricular cartilage creates channels through which cells can migrate into the matrix. Human chondrocytes and bone marrow-derived mesenchymal stromal cells efficiently colonize elastin-treated scaffolds through these channels, restoring a glycosaminoglycan-rich matrix and improving mechanical properties while maintaining size and shape of the restored tissue. The scaffolds are also rapidly colonized by endogenous cartilage-forming cells in a subcutaneously implanted osteochondral biopsy model. Creating channels for cells in tissue matrices may be a broadly applicable strategy for recellularization and restoration of tissue function.

1. Introduction

Cartilage consists of a single cell type, the chondrocyte, embedded in a flexible yet sturdy matrix [1,2]. It lacks blood vessels, nerves, as well as lymphatics, and in adults heals poorly after injury [1]. The combination of perceived structural simplicity and substantial clinical demand has made a prime tissue-engineering target for scientists. However, the mechanical characteristics of cartilage result from a complex matrix architecture that has been challenging to replicate [2–4].

One experimental approach to engineering tissue with the mechanical characteristics of cartilage has been to introduce chondrogenic cells into decellularized allogeneic or xenogeneic cartilage. Not only would this yield a scaffold with low immunogenicity, but the native cartilage environment may promote chondrogenesis in the newly introduced cells and thus facilitate restoration of the mechanical properties [reviewed in [5]]. Multiple protocols to remove cells from cartilage, using enzymes, detergents, denaturing chemicals, physical forces and combinations thereof have been developed [6–12]. However, the dense cartilage matrix has impeded the migration of cells into decellularized cartilage [reviewed in [13]].

Here we explore whether specific structural features of auricular cartilage would allow the introduction of cells into the matrix. Hyaline cartilage as found in the trachea, ribs, nasal septum and joints consists of a dense uninterrupted collagen type II matrix. Elastic cartilage, as found in the epiglottis, outer ear and eustachian tubes, contains a collagen type II matrix but is additionally traversed by elastin fibre bundles [1]. Due to the high prevalence of joint defects and the severity of tracheal injury, most research has focussed on the decellularization of hyaline cartilage. In this work, we aim to show that removal of the elastic fibre bundles traversing elastic cartilage generates channels through which cells can access the inner matrix and secrete glycosaminoglycans *in situ*, generating a cartilage-like tissue.

2. Materials and Methods

2.1 Decellularization with Elastase

Auricular cartilage was harvested from the ears of a human donor post-mortem [age 64] (body donation to Erasmus MC) or bovine calves [age: < eight months] (T. Boer & Zn. Nieuwerkerk aan den IJssel, the Netherlands). After washing the ears with water,

skin and muscle tissue were removed with a scalpel. Biopsies were taken using ∅6 or ∅8 mm biopsies punches (Stiefel Laboratories Nederland, Zeist, the Netherlands) and, where indicated, the perichondrium was removed using a scalpel. Subsequently, the cartilage was washed three times with deionized water (ISO 3696 Grade I), three times freeze-thawed in deionized water [-80°C to 37°C] and subsequently sterilized by incubation in 5% H_2O_2 (Sigma-Aldrich, Zwijndrecht, the Netherlands) at 37°C for at least one hour. The cartilage was then rinsed three times with sterile deionized water for five minutes and incubated for 24 hours rotating at 37°C in elastase solution: 3 units [Type IV] (Sigma-Aldrich) or 10 units (Gold Biotechnology Inc., St. Louis, USA) porcine pancreatic elastase per ml of 0.2 M tris(hydroxymethyl)-aminomethane [TRIS] HCl (Sigma-Aldrich) in water, set to a pH of 8.6. After elastase treatment, scaffolds were washed three times in sterile deionized water for five minutes. To hasten removal of cell debris, cartilage was exposed to physical strain: a snap freeze-thaw cycle [-190°C to 37°C], two eight-minute sonication rounds at 42 kHz [70-Watt water bath sonicator] and vortexing three times, in absence of liquid, for about 30 seconds at 2,500 RPM. Scaffolds were stored in sterile deionized water at -20°C until further processing. Matristypt™ collagen meshes (Dr Sulawek Skin & Healthcare AG, Billerbeck, Germany) were used as control scaffolds for cell seeding.

To test sterility of the decellularized cartilage, samples were incubated in MEM-α [Gibco brand] (Thermo-Fisher, Waltham, US) containing 10% heat-inactivated foetal calf serum [FCS] (Lonza, Basel, Switzerland) for 24 hours at 37°C, rotating at 30 RPM. Afterwards presence of bacteria and fungi was evaluated by light microscopy and unsterile samples were discarded.

2.2 Cell Sourcing and Culture

2.2.1 Bone Marrow-derived Multipotent Stem Cells

Human bone marrow-derived multipotent stem cells [BMSCs] were isolated from femoral marrow aspirates of adults undergoing total hip replacement (MEC-2004-142 & MEC-2015-644; age: 49-71; informed consent provided) or left-over iliac crest bone chips of children undergoing palate cleft reconstruction (MEC-2014-16; age: 9-13; implicit consent). Bone chips were swirled twice in 10 ml expansion medium and the medium than plated in 175cm^2 culture flasks, whereas bone marrow aspirates were diluted with expansion medium to 20 ml and plated in 175 cm^2 culture flasks. BMSCs expansion medium consisted of: MEM-α (Thermo-Fisher), containing 10% heat-inactivated FCS [Gibco brand] (Thermo-Fisher), 50 µg/mL gentamicin [Invitrogen Life Technologies brand] (Thermo-Fisher), 1.5 µg/ml amphotericin B [Fungizone™] (Thermo-Fisher), 0.1 mM L-ascorbic acid 2-phosphate and 1 ng/mL basic Fibroblast Growth Factor 2 [FGF2] (R&D Systems, Minneapolis, USA). After 24 hours, the flasks were gently washed with PBS containing 1% FCS and adherent cells expanded in expansion medium (refreshed every three days) till ca. 80% confluence. Afterwards cells were passaged to 2,300 cells/cm^2 into expansion medium with 250 ng/ml WNT3A, made in house by genetically modified Schneider *Drosophila melanogaster* S2 cells and purified as previously described [14]. Medium was refreshed daily and cells passaged once cells reached ca. 80% confluence. BMSCs were used for recellularization at passages two to four.

2.2.2 Articular Chondrocytes Sourcing and Culture

Human articular chondrocytes (ACs) were isolated from knee joints of patients undergoing total knee replacement (MEC-2011-371 [surgical waste material], age: 58-

68). Small chips were cut from macroscopically healthy areas of the cartilage using a scalpel and rinsed twice in PBS. The chips were then digested for 1 hour with 2 mg/ml protease (Sigma-Aldrich) in PBS followed by 0.5 mg/ml collagenase B (Roche Diagnostics, Rotkreuz, Switzerland) in DMEM (Lonza) with 10% heat-inactivated FCS (Thermo-Fisher) gentamicin [50 µg/mL] (Thermo-Fisher), and 1.5 µg/mL amphotericin B [Fungizone™] (Thermo-Fisher), rotating for at least twelve hours at 37°C. Afterwards, the solution was filtered through a 100 µm strainer (BD Biosciences, Franklin Lakes, USA), centrifuged, and the pellet washed twice in PBS. Chondrocytes were then plated at 7,500 cells/cm^2, expanded in the above mentioned DMEM-based medium (refreshed twice a week) and passaged when 80% confluence was reached. Chondrocytes were used for recellularization after one or two passages.

2.3 Cell Seeding

2.3.1 Onto the Scaffold Surface

Scaffolds without perichondrium were placed in the lids of 2 ml polypropylene microcentrifuge tubes (Thermo-Fisher) to ensure that seeded cells would settle on the scaffold only. Per mm^3 of sample, ca. 8,500 BMSCs or ACs were seeded statically, unless otherwise indicated, in the appropriate expansion medium (see above) and incubated in the inverted tubes for 24 hours at 37°C. When bilateral seeding was desired, scaffolds were turned after ca. twelve hours. Afterwards samples were transferred into 1/2 cm^2 wells of 48/24-well cell culture plates. To compare static and rotating seeding, scaffolds were placed into 2 ml polypropylene microcentrifuge tubes filled with cell suspensions of the indicated cell concentrations and incubated at 37°C either statically or rotating at a 45° angle.

2.3.2 Injection into the Scaffolds

For scaffolds with perichondrium, the ∅8 mm scaffolds were held tightly with tweezers and a concentrated cell suspension of less than 100 µl injected using a 27-gauge needle at three points (total ca. 8,500 cells/mm^3 scaffold volume). The scaffolds were then washed twice in PBS to remove cells on the surface and transferred to 2-4 cm^2 wells of 24/12-well cell culture plates.

2.4 Pellet-based Chondrogenicity Assay and Chondrogenic Differentiation

To evaluate chondrogenic differentiation potential, at least three pellets from each donor were formed by centrifuging 200,000 BMSCs or ACs in conical non-adherent polypropylene 15 ml tubes (Thermo-Fisher) at 300 g for eight minutes. Pellets were then cultured in 0.5 ml/tube chondrogenic differentiation medium; recellularized cartilage in 0.5 to 2 ml depending on volume. Chondrogenic differentiation medium contained: high glucose DMEM [Gibco GlutaMAX+] (Thermo-Fisher), 1:100 ITS+ plus mix [insulin, transferrin and selenous acid] (BD Biosciences), 40 µg/ml L-proline (Sigma-Aldrich), 1 mM sodium pyruvate (Thermo-Fisher), 10 ng/ml TGF-β1 (R&D Systems), 1.5 µg/mL amphotericin B [Fungizone™] (Thermo-Fisher) and 50 µg/ml gentamicin (Thermo-Fisher). For BMSC chondrogenic differentiation 100 nM dexamethasone (Sigma-Aldrich) was added [15]. Medium was refreshed twice a week for 35 days, after which the samples were harvested, rinsed in PBS and fixed in 4% formalin for 24 hours.

2.5 Migration Assays

2.5.1Migration in Response to a Serum Gradient

To serve as a serum reservoir, two ∅8 mm Matristypt™ collagen meshes (Dr Sulawek Skin & Healthcare AG) were placed at the bottom of 0.33 cm^2 wells (96 well plate). Then 15 µl FCS (Lonza) or 15 µl BMSC expansion medium were added to the meshes and allowed to soak in. Onto the collagen meshes, 1 mm thick, ∅8 mm elastase-treated auricular cartilage scaffolds were stacked and the 150 µl expansion medium without or with 10% FCS respectively added. Subsequently, ca. 2,500 cells/mm^2 were added into the well and allowed to settle onto the scaffolds. Since the diameter of the scaffolds was ca. 1 mm larger than that of the well, the scaffolds sealed the collagen meshes off, limiting cell migration to the cartilage. Scaffolds were then incubated for six days before harvest and processed as paraffin block sections, described below.

2.5.2 Migration in Serum-containing versus TGFβ1-containing Media

BMSCs were unilaterally seeded at 2,500 cells/mm^2 onto ca. 1 mm deep, ∅8 mm elastase-treated auricular cartilage scaffolds without perichondrium. The seeded scaffolds were cultured in either the serum-free, TGF*β*1-containing medium we used for chondrogenic differentiation of BMSCs (chondrogenic medium, see above) with the serum-containing or the TGF*β*1-free medium used for BMSC expansion (expansion medium). The scaffolds were incubated statically at 37°C and the appropriate medium refreshed daily. To visualize viable cells, on the day of harvest (one day or three days after seeding) Calcein AM (Thermo-Fisher) was added into the medium to 0.5 µM and the samples incubated for 30 minutes at 37°C in the dark. Subsequently, scaffolds were washed in PBS, harvested and then processed as cryosections as described below.

2.6 Articular Joint Defect Model

To evaluate articular cartilage defect closure we used a bovine osteochondral biopsy model system, developed previously by our lab [16,17]. In brief, we employed a hollow drill (DePuy Synthes, Palm Beach Gardens, USA) to create ∅8 mm osteochondral biopsies of four proximal sesamoid bones from fresh metacarpophalangeal joints from calves [age <8 months] (T. Boer & Zn.). The biopsies were rinsed twice with saline, then cut to about 5 mm in length and incubated overnight in full expansion medium. Using a ∅6 mm dermal biopsy punch (Stiefel Laboratories) and a scalpel, chondral or osteochondral defects were created. The defects were then washed twice in saline and ∅6 mm elastase-treated auricular cartilage scaffolds of ca. 0.7-1 mm [chondral] or 1.2-1.5 mm [osteochondral] height placed into the defects. The cartilage side of each biopsy was covered with an ∅8 mm Neuro-Patch™ membrane (B. Braun AG, Melsungen, Germany) to prevent murine tissue ingrowth. The samples were incubated for less than two hours in expansion medium until subcutaneous implantation into female NMRI nu/nu mice [ethical approval: DEC EMC3284] (Taconic Biomedical, Rensselaer, USA). Handling and housing of the mice was carried out in accordance with the EU Directive 2010/63/EU for animal experiments, with at least two mice housed together in one cage. Per mouse, four randomized chondral or osteochondral biopsies were implanted under isoflurane anaesthesia. In total n=12 elastase-treated auricular cartilage scaffolds were transplanted into n=4 chondral and n=8 osteochondral biopsies, distributed over two experiments with n=4 and n=6 mice respectively. Mice received 0.05 mg/kg bodyweight of Temgesic (Reckitt Benckiser, Slough, UK) one hour before and six to ten hours after surgery and 25 mg/kg bodyweight of amoxicilline (Dopharma Nederland, Raamsdonksveer, the Netherlands) during surgery. After two, four or ten weeks as indicated mice were euthanized by cervical dislocation. Cylinders were carefully explanted, surrounding tissue inspected

for macroscopic signs of inflammation and damage, fixed in 4% formalin for five days, subsequently decalcified using 10% formic acid (Sigma-Aldrich) for two weeks and embedded in paraffin.

2.7 Histological and Immunohistochemical Stainings

Paraffin embedded samples were sectioned at 6 µm thickness, placed on glass slides, dried and rehydrated. Frozen samples were sectioned at 10 µm thickness, frozen for at least 24 hours, then slowly thawed, air-dried and fixed using 100% acetone (Sigma-Aldrich). Both cryosections and paraffin block sections were stained with Haematoxylin (Sigma-Aldrich) and 2% Eosin (Merck Group, Darmstadt, Germany), 0.04% Thionin solution (Sigma-Aldrich) or Resorcin-Fuchsin solution [Klinipath brand] (VWR International, Breda, the Netherlands) according to manufacturer's instruction. Sections were subsequently dehydrated by increasing concentrations of ethanol (Sigma-Aldrich) and Xylene (Sigma-Aldrich) and sealed under a glass coverslip with PERTEX™ (HistoLab Products, Askim, Sweden).

For elastin staining, sections were incubated in 0.25% trypsin dissolved in PBS for 20 minutes at 37°C. Subsequently, non-specific binding sites were blocked with 10% goat serum in PBS and sections were stained for one hour with a monoclonal anti-elastin antibody [BA-4] (Sigma) diluted to 10 ug/ml in PBS. Sections were then incubated for 30 minutes at room temperature with an anti-mouse biotin labelled antibody diluted 1:50 in PBS with 5% FCS. Afterwards, sections were incubated for 30 minutes at room temperature with HRP–streptavidin conjugate (Biogenex, California, USA) diluted 1:50 in PBS/1% BSA. Labelling was detected using enzymatic turnover of a Neu Fuchsin substrate (Chroma, Köngen, Germany). Sections were then airdried overnight and

sealed under a glass coverslip with Vectamount [#H5000] (Vector Laboratories, Burlingame, USA).

2.8 Imaging, Cell Migration and Cell Density Quantification

Stained sections were imaged using cellSens™ Standard software (Olympus Europe, Hamburg, Germany) with a 5-megapixel digital 14-bit colour camera [model UC50] (Olympus Europe) attached to an upright light microscope for slides [model BX 40] (Olympus Europe). Cell migration distance was measured by creating bins of 250 µm height and 2,250 µm width (0.5 mm^2) with the linear measurement tool in cellSens™ and cell numbers were counted manually in ImageJ (NIH, Bethesda, USA) [18]. The first 25 µm from the cartilage surface were excluded to discount cells adherent but not migrating. Cell density was determined by counting cells per 0.1 mm^2 field, with six (seeding) or twelve (injection) fields per sample and depth. Cell distance distribution was determined by measuring n=60 nuclei-nuclei distances per donor on H&E, excluding cells sharing lacunae or within 25 µm of the scaffold surface. The maximum width of cell distributions for an injection side was determined by measuring the distance between the cells furthest apart either perpendicular or parallel to the perichondrium in six different areas per sample. All quantification of cell numbers was performed blinded by one person (J.L.), with the exception of supplementary figure 2(b), which was scored unblinded.

2.9 Mechanical Testing of Native, Elastase-treated and Recellularized Cartilage

Nanoindentation of bovine auricular cartilage scaffolds was performed using a displacement-controlled nanoindenter [model name Piuma] (Optics11, Amsterdam, the Netherlands) with a spherical probe [stiffness: 58.3 N/m; radius: 51 µm] using a measurement protocol based on Moshtagh [19]. Force-displacement curves were

generated based on cantilever deflection and indentation depth as controlled by a piezoelectric motor. For indentation, each cartilage biopsy was submerged in PBS within a glass petridish, held in place by an agarose mould. The probe was calibrated and then for each scaffold a square matrix of 16 indentation points [250 µm apart] were measured. For each indentation, the probe was held above the surface for 0.5 seconds, followed by indentation to 15 µm for 1 second, holding the probe at 15 µm seven seconds, unloading over 20 seconds and then pausing for 0.5 seconds prior to moving to the next indentation point. The Piuma software (Optics11) then calculated the effective elastic modulus based on the slope of the stress-strain curve using the Oliver-Pharr theory[19] Minimal variability between different measurement sessions was ensured by indenting a set [n=3] of control scaffolds (decellularized, untreated) during every session. Since removal of elastin with elastase can dramatically alter the viscoelastic behaviour of auricular cartilage [20], we refer to the measured values as stress-strain modulus. In total 8x untreated, 10x decellularized and 44x recellularized (>3 per donor) cartilage scaffolds were indented.

2.10 Statistics

Analysis of numerical data was performed in SPSS 20 (IBM, North Castle, USA). Migration in expansion and chondrogenic medium were compared pairwise for day three using the Mann-Whitney-U test. Migration into different depths in presence and absence of serum were tested, paired by depth, using the Wilcoxon signed-rank test. The stress-strain modulus values were compared pairwise for all samples using the Kruskal-Wallis Test (indicated significance is for the pairwise comparison of all scaffolds to decellularized-only scaffolds). We set p=0.05 as cut-off for significant

differences for all tests, with the p-values given in the figure legends (rounded up if $p<0.01$).

3. Results

3.1 Recellularization of auricular cartilage after removal of elastin fibres

To determine if removal of elastin permits recellularization of cartilage, we digested elastin in devitalized bovine auricular cartilage scaffolds by treatment with 3 U/ml pancreatic elastase for 24 hours. Staining with resorcin-fuchsin showed that the treatment removed elastin fibres, opening the otherwise dense pericellular matrix containing the chondrocytes (lacunae) and leaving behind channels traversing the collagen network (figure 1(a)). The elastase treatment was also sufficient to remove most cell remnants and deplete glycosaminoglycans (figure 1(b)). Elastin depletion was elastase dose-dependent, with 3 to 10 U/ml (brand-dependent) elastase completely depleting elastin fibres as detected by resorcin-fuchsin staining in bovine auricular cartilage (supplementary figure 1(a), (b)). To confirm depletion of elastin seen on resorcin-fuchsin staining, we performed immunohistochemistry with a monoclonal elastin-specific antibody ((supplementary figure 1(c)). Moreover, loss of glycosaminoglycans, as indicated by thionin staining, as well as cell remnants, visible on thionin and H&E stainings, were associated with elastin depletion (supplementary figure 1(a), (b)). Elastase treatment was equally efficient in clearing elastin in human and bovine auricular cartilage, but glycosaminoglycan depletion required higher elastase concentrations in human compared to bovine cartilage (supplementary figure 1(d), (e)). Overall, elastase treatment renders bovine and human auricular cartilage porous, decellularizes it and depletes glycosaminoglycans.

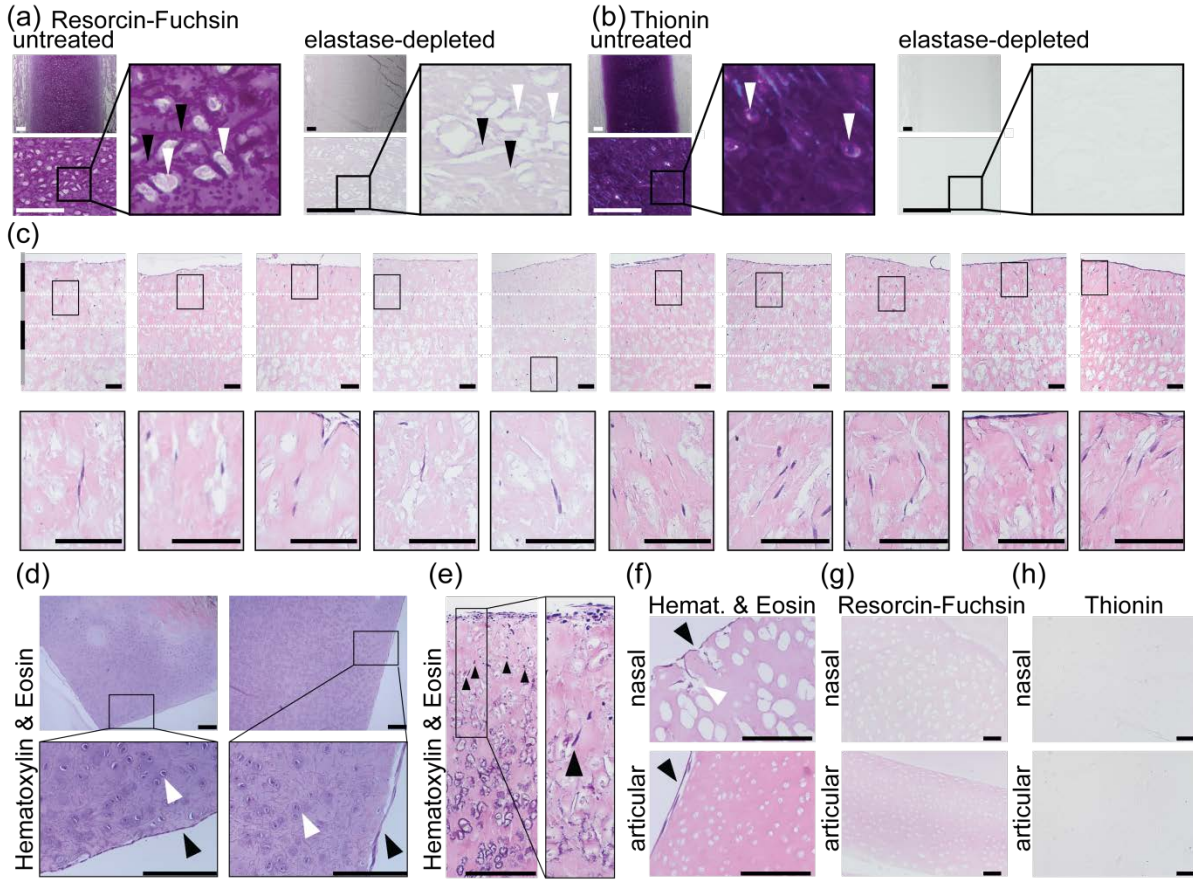

Figure 1. Elastase treatment removes elastin fibres and glycosaminoglycans, permitting recellularization. (a, b) Bovine auricular cartilage before and after treatment with elastase, stained with (a) resorcin-fuchsin (highlights elastic fibres) or (b) thionin (marking glycosaminoglycans). Scale bars = 200 µm. White arrowheads indicate lacunae where cells are/were located in, black arrowheads elastin fibre bundles/channels. (c) Bovine auricular cartilage treated with elastase stained with haematoxylin and eosin (H&E) six days after being unilaterally seeded with BMSCs. Cells tunnelling through the channels left behind after elastin fibre removal are highlighted in the insets. Scale bars = 100 µm; horizontal dotted white lines in (c) ca. 200 µm, 400 µm and 600 µm from seeded surface. (d) H&E staining of two bovine auricular cartilage scaffolds not exposed to elastase but undergoing all other steps of the decellularization protocol and then cultured for six days after seeding with BMSCs. Magnified panels show nuclei of resident chondrocytes (white arrowheads) remaining in the matrix and seeded BMSCs (black arrowheads) not invading. Scale bars = 200 µm. (e) H&E staining of a bovine auricular cartilage scaffold treated with 0.1 U/ml elastase to partially remove elastin and then cultured for six days after seeding with BMSCs. Black arrowheads indicate cells that have entered the matrix furthest. Scale bar = 200 µm (f)H&E staining showing cells adherent to elastase-

treated bovine articular and nasal cartilage scaffolds cultured for six days after seeding with BMSCs. Black arrowheads highlight cells incapable of invading the articular and nasal cartilage matrix. Highlighted by a white arrowhead are cells that invaded the lacunae cut open during processing but did not migrate further into the scaffold. Scale bars = 200 µm. . (g, h) Depletion of glycosaminoglycans and lack of elastin fibres visible on (g) rescorcin-fuchsin and (h) thionin stained elastase treated bovine articular and nasal cartilage scaffolds. Scale bars = 200 um.

To determine if the channels created by elastase treatment allowed cell migration, we seeded the elastase-treated auricular cartilage scaffolds with 8,500 human bone marrow-derived multipotent stem cells [BMSCs] (expanded for two to three passages with WNT3A and FGF2) per mm^3 scaffold. BMSCs are attractive for articular cartilage repair, since they are highly chondrogenic they can be expanded, and the donor site morbidity caused by bone marrow aspiration is limited [21]. We have previously shown that culturing with WNT3A and FGF2 maintains BMSC's chondrogenic capacity during expansion [22]. The ca. 1 mm thick scaffolds were seeded unilaterally for 24 hours, leading to the deposition of cell layers on the scaffold surface. We sectioned scaffolds six days after seeding with BMSCs to investigate the extent of cell invasion (figure 1(c)). We found that cells invaded the scaffolds with 53 ± 15% of invading cells having migrated up to 200 µm from the surface, 25 ± 4% 200 to 400 µm, 14 ± 9% 400 to 600 µm and 7 ± 8% 600 to 800 µm. Cells that invaded were frequently found stretched within the channels, radiating from the seeding surface, indicating migration along the voids created by elastin fibre removal (figure 1(c)). On the other hand, bovine auricular cartilage not treated with elastase and therefore lacking channels, was not invaded by cells (figure 1(d)). Moreover, when exposure to elastase was limited and therefore elastin only removed from part of the biopsy, cell invasion was limited to areas where elastin fibres were cleared (figure 1(e)). This suggests that removal of elastin by

elastase treatment is responsible for rendering auricular cartilage permeable to cells. To further confirm that elastase allowed recellularization by removing elastin fibre bundles, we treated bovine nasal and articular cartilage, which are hyaline and lack elastin fibre bundles, with elastase. While this depleted glycosaminoglycans from both nasal and articular cartilage, no visible channels formed, and cells did not invade into the matrix (figure 1(f)-(h)). In summary, this indicates removal of elastin fibre bundles allows cells to invade auricular cartilage.

3.2 Static Seeding and Chondrogenic Differentiation Conditions Facilitate Uniform Recellularization of Elastase-treated Auricular Cartilage

We observed that the number of cells invading the scaffold correlated with the number of cells on the closest scaffold surface. We therefore compared static and rotating seeding at different cell concentrations to identify under which condition cells adhered densely and uniformly to the scaffold surface. Rotating the scaffolds continuously or intermittently during seeding induced cell clumping as well as irregular seeding and was not further explored. Maintaining a consistent total seeded cell number, we found that a 500 cells/µl suspension yielded a good combination of cell density and uniformity, with other concentrations yielding significantly lower cell densities or showing large sample variation (supplementary figure 2(a), (b)). Exposing the scaffold to the cell suspension for longer than 24 hours did not yield higher cell densities [data not shown]. BMSCs remained viable and attached to the scaffold throughout a culture period of at least 30 days (supplementary figure 2(c)). Culture-expanded chondrocytes also allow generation of autologous cartilage, and might be favourable for small defects or when donor site morbidity is not of concern (e.g. in microtia, where cells can be derived from

the to-be-reconstructed malformed auricle) [23–25]. Expanded, dedifferentiated adult human articular chondrocytes (ACs) adhered well to elastase-treated auricular cartilage and remained viable for at least 30 days (supplementary figure 2(d), offering an alternative to BMSCs. Given that 24-hour seeding with 500 cells/µl yielded a high average cell density with low variation, we continued with this set-up for all subsequent experiments.

We observe that cell density within the scaffold declined with distance to the seeding surface (figure 1(c)). BMSCs and chondrocytes migrate towards attractants contained in foetal calf serum [26,27]. We therefore tested whether a serum gradient encouraged BMSCs migration by placing a serum-laden sponge against the scaffolds, opposite to the cell seeding surface. The serum gradient significantly increased the number of BMSCs migrating into the tissue (figure 2(a)). Notwithstanding, distribution of cells within the scaffolds remained skewed towards areas within 500 µm of the seeding surface.

In vivo, transforming growth factor 1 beta (TGFβ1) stimulates migration of BMSCs through tissues [28,29]. TGFβ1 also induces chondrogenic differentiation in BMSCs and de-differentiated chondrocytes [15,30,31], which is required to restore the decellularized matrix. Because chondrogenic medium may thus enhance both migration of seeded cells and matrix regeneration, we compared migration in a serum-free, TGFβ1-containing medium commonly used for chondrogenic differentiation of BMSCs [15] (chondrogenic medium) with the serum-containing, TGFβ1-free medium we used for BMSC expansion (expansion medium). Three days after seeding, significantly more BMSCs (2.9 ± 0.7-fold increase) migrated into the scaffolds in chondrogenic compared to expansion medium (figure 2(b), (c)).

Since BMSCs migrated through the scaffold in chondrogenic medium, we assessed if in a timeframe sufficient for chondrogenic differentiation and matrix synthesis *in vitro* (35 days) [22], BMSCs would recellularize the scaffolds to cell densities comparable to native cartilage. Scaffolds (height 1mm, ∅8 mm, ca. 50 mm^3) were seeded with 450,000 BMSCs and cell density quantified on H&E stained 6 µm sections after 35 days culture in chondrogenic medium. Cell density averaged 150 cells/mm^2 and varied little between BMSC donors (figure 2(d)). The average cell density of recellularized scaffolds was lower than that of native bovine (239 ± 53 cells/mm^2) or human (306 ± 67 cells/mm^2) auricular cartilage as well as that of human septal nasal cartilage (226 cells/mm^2) [32], but higher than that of human femoral condylar articular (layer dependently 32-76 cells/mm^2) [33] or costal cartilage (27 cells/mm^2) [33] (figure 2(d)). Cell density was slightly higher near the seeding surface, with the innermost areas containing on average 23% less cells than areas below the surface. Average cell-cell distance in the recellularized scaffolds was 63 ± 28 µm, slightly higher than the 57 ± 21 µm in native bovine auricular cartilage (supplementary figure 3(a)). These findings indicate that BMSCs recellularize the elastase-treated auricular cartilage scaffolds to levels comparable to native cell density and distribution.

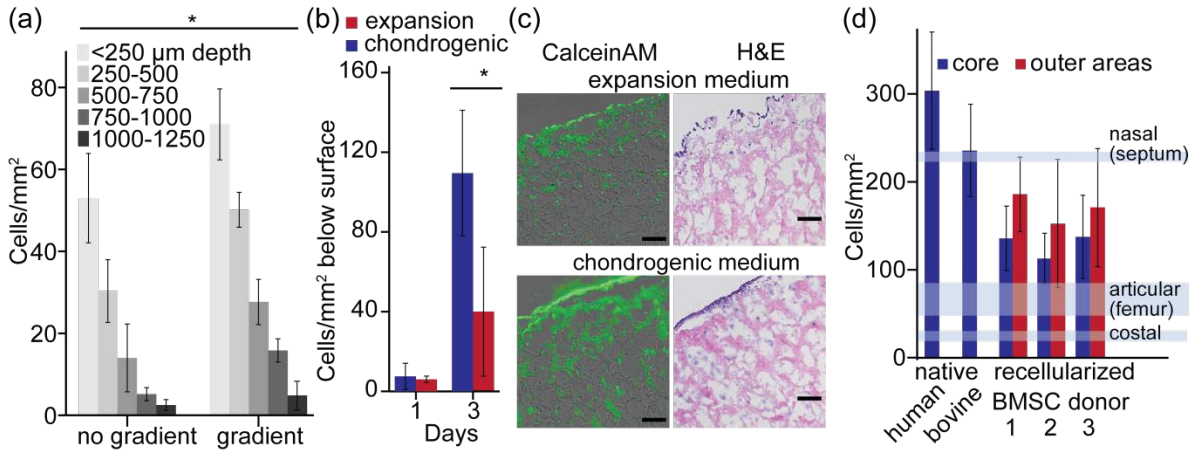

Fig. 2 In chondrogenic differentiation conditions cells rapidly distribute through the matrix to near native densities. (a) Plot showing the number of BMSCs that have migrated into zones at different depths from the seeding surface after six days culture in DMEM with 10% serum on both sides of the scaffold (no gradient) or DMEM with no serum and an 10%-equivalent volume serum on the side opposite of the cells (gradient). For each of n=3 samples per depth the counts of four 100µm-apart sections were averaged. Error bars = SD. * p <0.01 (Wilcoxon signed-rank test, paired by depth). (b) Plot showing the number of BMSCs that have migrated into the scaffold (>25 µm from scaffold surface) after one- or three-days of culture in chondrogenic or expansion medium. n=4 scaffolds, error bars = SD, Mann-Whitney-U test, 2-tailed significance * p=0.03. (c) Representative micrographs of day three samples from (b) stained with CalceinAM to mark live cells and merged with brightfield images to show matrix boundaries or stained with H&E. Scale bars = 100 µm. (d) Cells per mm^2 plotted for native bovine and human auricular cartilage as well as elastase-treated bovine auricular cartilage scaffolds superficially seeded with BMSCs and cultured 35 days culture in chondrogenic medium. For each of the three donors six non-overlapping fields of 0.1 mm^2 were counted for the core (inner 250 um) or in the outer areas (>25 µm from surface) of the scaffold. Error bars = SD. Blue bars indicate cell densities from literature for human nasal [32], articular (range of all depths) [33] as well as costal cartilage [33].

3.3 Overcoming the Perichondral Barrier by Cell Injection

Plastic surgery of the auricle (outer ear), the nasal septum or alar nasi is one area where auricular cartilage matrix scaffolds could be employed. Since these cartilage structures are lined by perichondrium which contributes to integration with the

surrounding tissues as well as to mechanical properties of the structure, we studied grafts with perichondrium intact. However, in the cellular (cambium) layer of the perichondrium surrounding the auricular cartilage that lacks elastin fibres (figure 3(a)), no channels formed after elastase treatment (figure 3(b)). Furthermore, no cells could be detected in the cambium layer or the underlying cartilage after recellularization (figure 3(c)). However, when the perichondrium was removed from one side prior to recellularization, cells were observed below the cambium layer on the other side (figure 3(d)), showing that the seeded cells were able to migrate to the cambium layer but could not cross the perichondrium. To find a method to recellularize full thickness cartilage, we assessed whether BMSCs would distribute throughout the matrix upon injection into scaffolds without removal of the perichondrium. Histology indicated that the matrix was minimally distorted after injection, with visible damage far smaller than the needle diameter (figure 3(e)). As with superficial seeding, we compared cell migration in chondrogenic with expansion medium. Six days after injection, BMSCs were found throughout the matrix surrounding the injection sites and average cell density at the centre of the scaffold was 193 ± 88 cells/mm^2 for culture in chondrogenic and 197 ± 80 cells/mm^2 for expansion medium (figure 3(f)). 800 μm from the centre of the scaffold, average cell density was 214 ± 124 cells/mm^2 for culture in chondrogenic and 168 ± 60 cells/mm^2 for expansion medium. There were no significant differences between either the media nor between central and peripheral areas within the scaffold (figure 3(f)). Overall cell density in scaffolds cultured in chondrogenic medium (193 ± 88 cells/mm^2) was not significantly different ($p = 0.24$, Mann-Whitney-U test) from that of native bovine auricular cartilage (239 ± 53 cells/mm^2), but significantly lower ($p < 0.01$) than native human auricular cartilage human (306 ± 67 cells/mm^2). Moreover,

cell density after injection for both media was higher than that of human costal and articular cartilage, but lower than that of human nasal septal cartilage (figure 3(f)).

To estimate what scaffold area would be recellularized per injection, we measured cell spread from visible injection sites on histology. Cells spread approximately 2 mm parallel to the perichondrium, with little difference between media (supplementary figure 3(b)). Perpendicular to the perichondrium cells spread 849 ± 174 µm in chondrogenic medium (covering 86% of the entire inter-perichondral distance of 997 ± 251 µm of those samples) and 871 ± 49 µm(representing 91% of the entire inter-perichondral distance of 953 ± 55 µm of those samples) in expansion medium (supplementary figure 3(c)). Together, these data indicate that injection of cells allows uniform recellularization of elastase-treated auricular cartilage scaffolds with intact perichondrium on both sides.

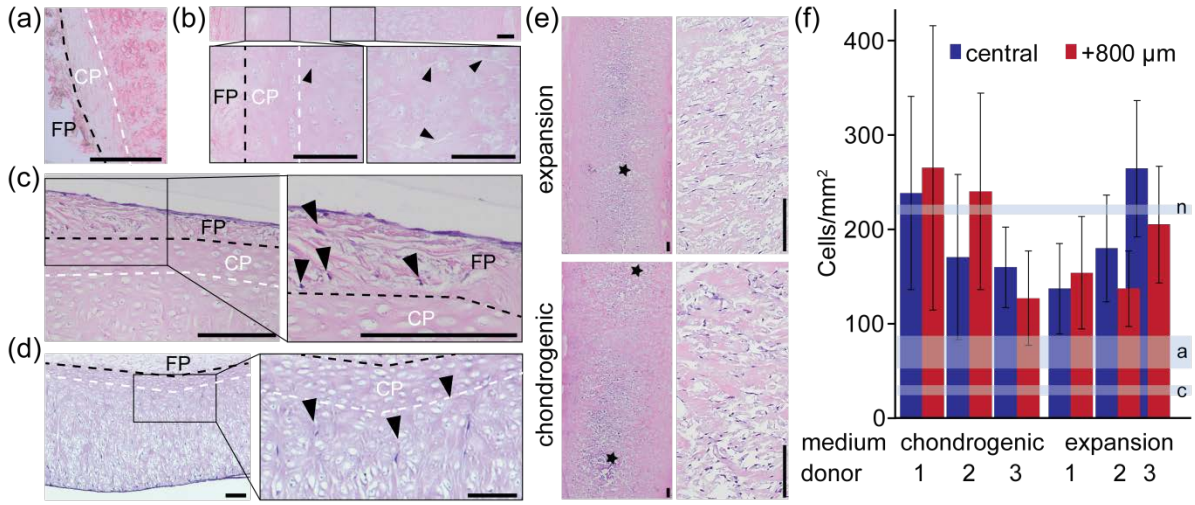

Figure 3 Prevention of cell invasion by perichondrium can be overcome by injecting cells.

(a) Fibrous (**FP**) and cambium layer (**CP**) of the perichondrium in a section of untreated bovine auricular cartilage stained for elastin. Dotted lines indicate borders between FP and CP (black) and CP and cartilage (white). (b) H&E staining of a full thickness elastase-treated bovine auricle with many channels present in the centre (black arrowheads) but not in the FP or CP. (c) H&E staining of elastase-treated auricular cartilage recellularized from the perichondrium side. Cells (black

arrowheads) adhere to and migrate into the FP, but do not cross into the underlying CP or cartilage. (d) H&E staining of elastase-treated auricular cartilage with perichondrium removed from one side (bottom) but left intact on the other side (top) after 21 days of recellularization from the side without perichondrium. Cells (black arrowheads) migrate through the matrix but stop where cartilage and CP meet. (e) H&E staining of full thickness (height >3mm, ∅ 8 mm) scaffolds injected with BMSCs and cultured six days culture in chondrogenic or expansion medium. Stars highlight injection sides, note that each scaffold was injected at three different points, but not all are visible in the sections shown. (f) Plot showing cells per mm^2 in scaffolds with intact perichondrium injected with BMSCs after six days culture in chondrogenic or expansion medium. For each of three scaffolds twelve non-overlapping 0.1 mm^2 fields were counted either on a section of the scaffold centre or a section 800 µm further towards the outer perimeter. Error bars = SD. Blue bars indicate cell densities from literature for human nasal (n) [32], articular (range of all depths) (a) [33] as well as costal (c) cartilage [33]. (a)-(e) Scale bars = 200 µm.

3.4 Restoration of glycosaminoglycans content and mechanical properties in a recellularized matrix that retains its size and shape

Synthetic collagen-based scaffolds have been explored for cartilage tissue engineering but frequently shrink and distort due to cell contractions, especially during chondrogenic differentiation [34,35]. To estimate scaffold contraction, we compared the size of untreated auricular cartilage scaffolds to elastase-treated scaffolds recellularized with BMSCs or culture expanded ACs and then cultured in chondrogenic differentiation medium. As a reference for cell contraction, we seeded the same number of cells from the same donors onto an equally-sized collagen mesh (Matristypt™) used for tissue engineering [36]. The auricular cartilage scaffolds retained their shape and size after elastase treatment and during chondrogenic differentiation of BMSC or ACs, while the collagen mesh shrank severely (figure 4(a)). The height of elastase-treated and recellularized scaffolds (827 ± 102 µm) was similar to that of untreated scaffolds (735 ± 22 µm) (figure 4(b)). This indicates that elastase-

treated auricular cartilage scaffolds resist distortion following reseeding and chondrogenic differentiation.

The unique compressibility of articular cartilage is explained largely by glycosaminoglycans attracting fluid while trapped within a collagen network [20]. These glycosaminoglycans are however removed by elastase treatment (supplementary figure 1(a), (b)). We therefore investigated whether reseeded cells would restore the glycosaminoglycans of the matrix. After chondrogenic differentiation for 35 days, both BMSCs (figure 4(c)) and expanded ACs (figure 4(d), (e)) secreted glycosaminoglycans into the surrounding matrix. Thionin staining was localised to areas near cells, indicating that glycosaminoglycans are produced by the seeded cells and that their mobility is limited (figure 4(c)). We tested, using nanoindentation, whether local restoration of glycosaminoglycans would also restore mechanical properties. The stress-strain modulus increased from 27 kPa in unseeded matrix to between 39 kPa and 64 kPa, depending on the BMSC donor used, after recellularization and chondrogenic differentiation, and was significant ($p<0.01$) for BMSCs from 9 out of 10 donors (figure 4(f)). Mechanical properties and glycosaminoglycan secretion varied considerably between donors, with highly-chondrogenic paediatric BMSCs [donor 1] showing the strongest thionin staining as well as the highest stress-strain modulus (figure 4(f), (g)). Although still significantly lower than the stress-strain modulus of 230 kPa for native bovine auricular cartilage (figure 4(f)), our findings suggest that restoration of glycosaminoglycans with recellularization promotes compression resistance of the elastase-treated auricular cartilage scaffolds, depending on the chondrogenic potential of the cells.

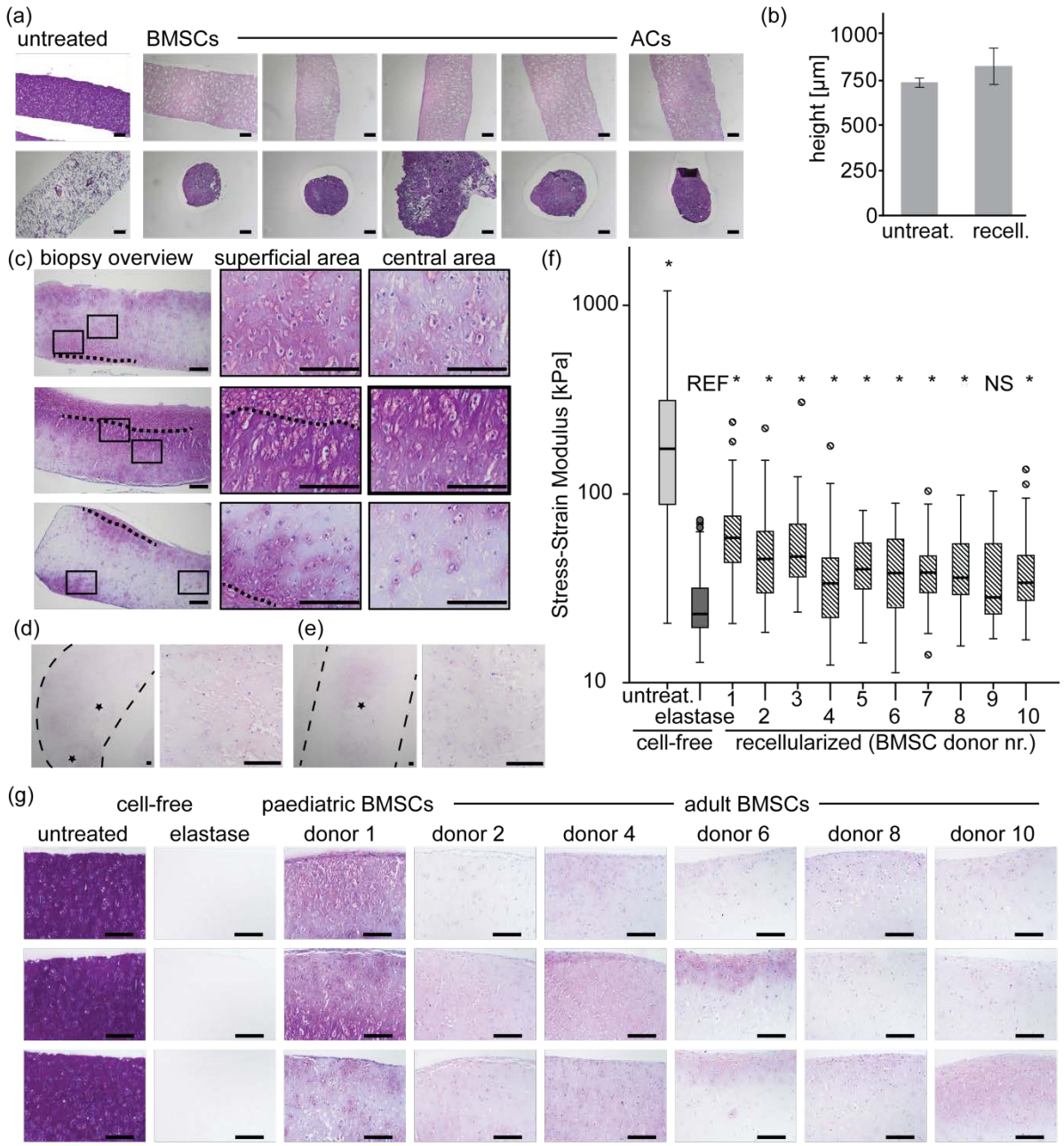

Figure 4. Elastase-treated auricular cartilage scaffolds retain size and shape and seeded cells restore glycosaminoglycans and mechanical properties. (a) H&E staining showing the full height of biopsies (∅6 mm) of bovine auricular cartilage (top row) and a collagen scaffold (Matristypt™) (bottom row) either untreated (first image) or seeded with 250,000 cells per sample (four different BMSC donors, one AC donor, matched in columns) and cultured for 35 days in chondrogenic medium. Scale bars = 200 µm. (b) Plot of mean height for three untreated bovine auricular cartilage and five recellularized, elastase-treated bovine auricular cartilage scaffolds after 30 days of culture. Per sample the shortest distance between the upper and lower sample sides was measured at

points 200 µm apart. Error bars = SD. (c) Stress-strain modulus determined by nanoindentation for untreated and elastase-treated bovine auricular cartilage as well as elastase-treated bovine auricular cartilage scaffolds recellularized with BMSCs from different donors and cultured in chondrogenic medium for 35 days. Values from a 16-point/sample indentation matrix for n=8 (untreated), n=10 (elastase-treated) and per donor n>3 (recellularized) scaffolds. Two-tailed, asymptotic Kruskal-Wallis Test: pairwise comparison to elastase-treated scaffolds, adjusted significance: * $p<0.01$. (d) Thionin staining of scaffolds reseeded with BMSCs and chondrogenically differentiated for 35 days. Three representative scaffolds with windows highlighting superficial and central areas. Dotted lines indicate the border between scaffold and new matrix generated by seeded cells *ex situ*. Scale bars = 200 µm. (e), (f) Thionin staining of scaffolds with intact perichondrium injected with ACs and chondrogenically differentiated for 35 days. Dotted lines indicate the cartilage outer border, stars highlight injection sites. (e) Central area of a sample sectioned parallel to the perichondrium, (f) central area of different sample cut perpendicularly to the perichondrium. Scale bars = 200 µm. (g) Thionin staining for untreated and elastase-treated bovine auricular cartilage as well as representative elastase-treated bovine auricular cartilage scaffolds recellularized with adult and paediatric BMSCs from different donors and cultured in chondrogenic medium for 35 days (donor numbering as (c)). Scale bars = 200 µm.

3.5 Chondrogenic cells invade elastase-treated auricular cartilage in vivo

So far, we have shown that elastase-treated auricular cartilage scaffolds are rapidly recellularized *in vitro*. However, in some clinical applications, such as articular cartilage repair using matrix assisted chondrogenesis in combination with microfracture, *in vivo* recellularization is possible [37] and favourable requiring only one surgery and no *in vitro* culture. We therefore investigated if elastase-treated auricular cartilage scaffolds would be recellularized *in vivo* in an established articular cartilage defect model [16,17,38]. Osteochondral and chondral defects in bovine metacarpophalangeal joint biopsies were filled with cell-free elastase-treated bovine auricular cartilage scaffolds of thickness matching the defect size and then transplanted under the skin of immunocompromised mice. In chondral defects, cells

from the surrounding bovine articular cartilage entered the borders of the scaffold over ten weeks and formed cartilage *de novo* within (figure 5(a)) or adjacent to the scaffold (figure 5(b)). The amount of glycosaminoglycan synthesis however differed considerably between samples and none showed complete defect closure within this time frame. In osteochondral defects, cells invading from the bone marrow side distributed throughout the scaffold and formed new cartilage *in situ* within four weeks, connecting the scaffold to the surrounding cartilage (figure 5(c), (d)). After ten weeks, the cartilage tended to become hypertrophic (figure 5(e)) and in some areas was replaced by marrow-containing bone (figure 5(f)). Whereas this led to restoration of the subchondral defect area, the bone-like tissue extended throughout the defect up to the articular cartilage level, conceivably because this model lacks synovial fluid and mechanical loading. In osteochondral defects not filled with a scaffold, neither hypertrophic cartilage nor bone formed, instead the subchondral area was distorted, and the defect was filled by mostly sparse fibrous tissue (figure 5(g)). These findings indicate that in a joint defect model, elastase-treated bovine auricular cartilage scaffolds are rapidly invaded by chondrogenic cells.

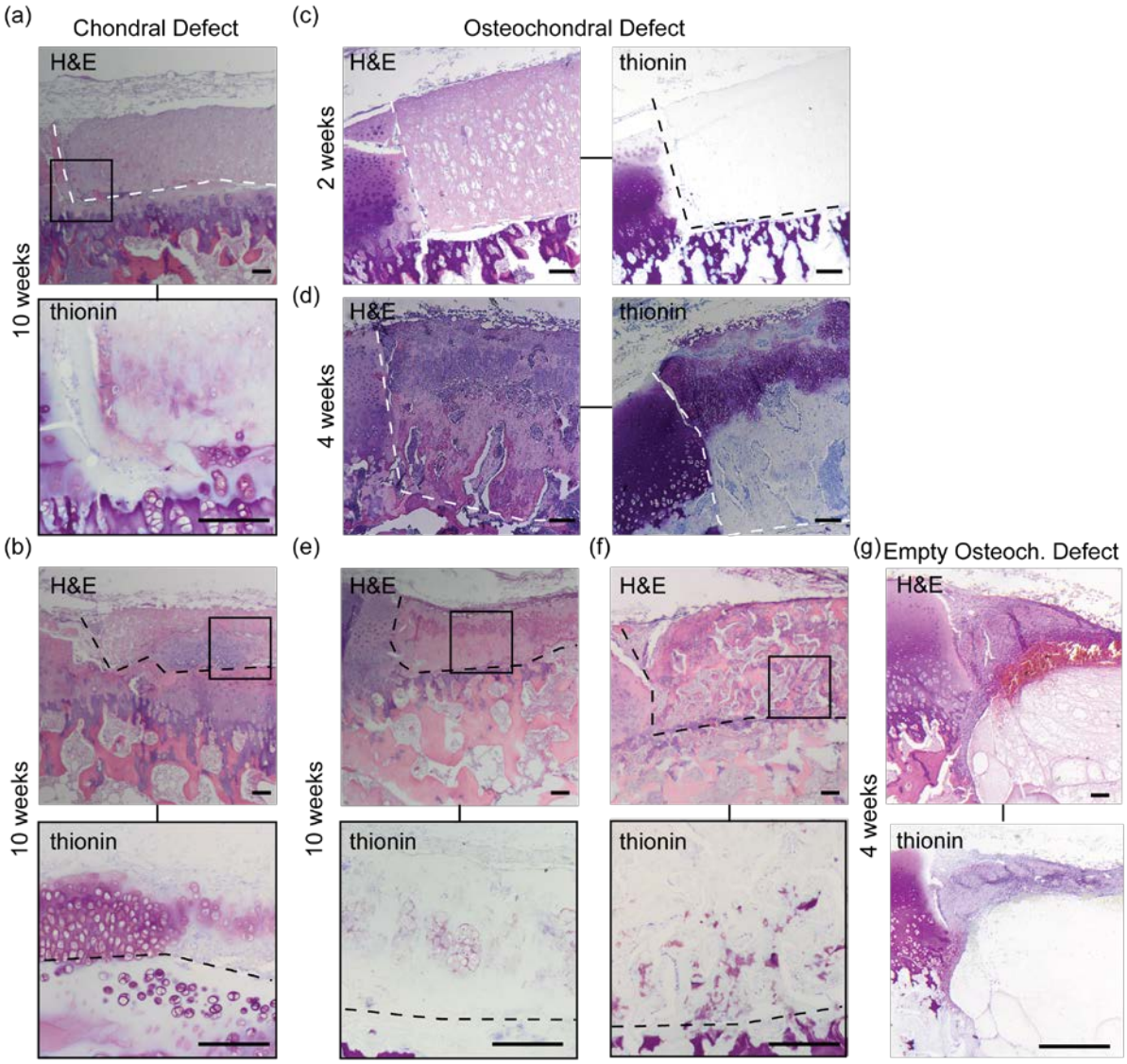

Figure 5. Chondrogenic cells invade the elastase-treated auricular cartilage scaffold in vivo. (a)-(f) H&E and thionin staining of defects in osteochondral biopsies taken from bovine metacarpophalangeal joints, filled with elastase-treated auricular cartilage scaffolds and implanted subcutaneously into immunodeficient mice. (a), (b) Chondral defects after ten weeks and (c) osteochondral defects after two weeks, (d) four weeks and (e)/(f) ten weeks. (g) A control osteochondral defect left empty and harvested after ten weeks *in vivo*. Insets showing magnified area from a consecutive section stained for thionin shown for (a), (b), (e) and (f). Dotted lines indicate defect borders, scale bars = 200 µm.

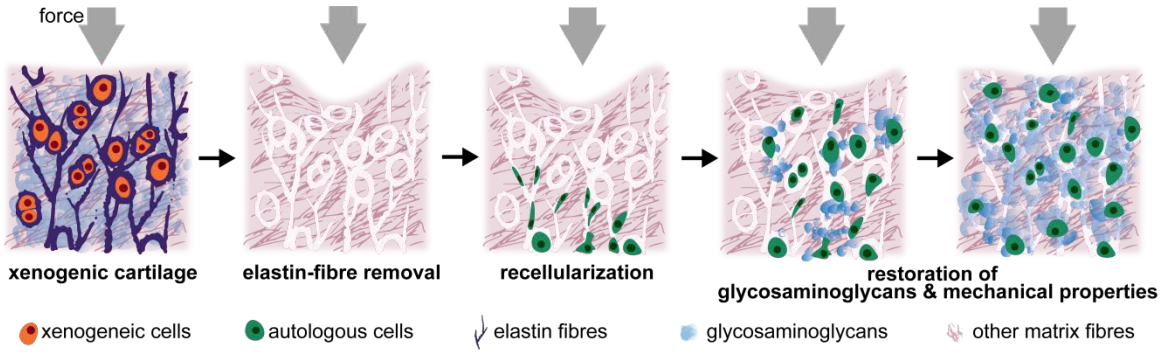

Figure 6. Schematic Representation of Recellularization via Elastase-Generated Channels

Elastase treatment of (xenogeneic) cartilage depletes elastin fibres as well as glycosaminoglycans from the matrix, resulting in a decrease in compression resistance, and facilitates removal of resident (xenogeneic) chondrocytes. Seeding of (autologous) chondrogenic cells then allows even recellularisation of the cartilage matrix via the channels left behind after elastin fibre removal. When induced to undergo chondrogenic differentiation, the invading cells rapidly generate new glycosaminoglycans within the matrix, partially restoring compression resistance.

4. Discussion

The dense matrix of cartilage is the principal hindrance to recellularization [13]. This study presents a method to make a cartilage-derived scaffold that is permeable to cells by the removal of elastin fibres from auricular cartilage (figure 6). We observed cells rapidly migrating along the channels left behind after elastin removal and distributing throughout the scaffold *in vitro* and *in vivo*. The invaded cells partially restored the glycosaminoglycans, with the scaffolds increasingly resembling cartilage in morphology and mechanics. While cartilage decellularization protocols permitting chondrogenesis of seeded cells have been reported previously, cell invasion was limited to less than 100 µm from the surface or perforations, presumably because migration occurred via lacunae that had been cut open [8,39]. Our work significantly expands the applicability of cartilage recellularization approaches. The channels we create by removing elastin fibres extend through the entire auricular cartilage with the

exception of the perichondrium, allowing cells to rapidly recellularize the complete tissue. Articular and nasal septum cartilage defects less than 3 mm thick could be filled with a single layer of elastase-treated bovine auricular cartilage [40,41]. In order to imitate the zonal architecture of articular cartilage, it may be possible to retard cell migration unilaterally by taking advantage of the decrease of elastin fibre density towards the perichondrium. The complex shapes of ear and tracheal cartilage or thicker articular cartilage defects would likely require combining multiple scaffolds.

While cartilage defects cause pain, they are, with the exception of those in the trachea, not life-threatening and thus rarely warrant the added risk inherent to immune suppression. We show that the scaffold can be derived from bovine or human auricular cartilage, with preliminary evidence indicating that the protocol is also applicable to porcine auricular cartilage [data not shown]. Elastase-treatment caused decellularization, which when combined with treatments to remove disease vectors and residual nucleic acids provides, in principle, non-immunogenic human allografts. Xenografts are not limited by donor material scarcity and the bovine auricle is considerably thicker and more plane than the human auricle, facilitating the design of larger scaffolds. While cellular bovine or porcine cartilage xenografts are immunogenic [42], xenogenic collagen matrices are routinely used for articular cartilage defect repair [43] and five decades of experience with porcine and bovine heart valves indicates that acellular xenografts have acceptable immunogenicity after reducing xenoantigens enzymatically [44]. Transplantation experiments in immunocompetent animals should be performed to confirm the low immunogenic nature of the decellularized scaffold before clinical application.

Getting sufficient chondrogenic donor cells is a bottleneck for cartilage tissue engineering [45]. It is thus an asset that few cells efficiently recellularize large areas

and continue to proliferate within the scaffold. Extrapolating from ca. 8,500 cells we seeded per mm^3 scaffold, a large 3 mm deep, 2.5 cm diameter (1470 mm^3) articular cartilage defect would require 12 x 10^6 BMSCs, a number we routinely gain from 15 ml bone marrow aspirates within ten days culture [22]. Similar numbers can be obtained for chondrocytes by expanding cells from a 1 mm diameter nasal septum biopsy [46] or directly from 7 g of articular cartilage [47]. Moreover, we show that elastase-treated auricular cartilage scaffold is directly suitable for defect shape-matched cell-free implantation, permitting *in vivo* recellularization. Once treated with elastase the scaffold can be stored frozen and then cut to size and used off-the-shelf in clinical scenarios where chondrogenic cells are accessible *in situ*, e.g. microfracture-based articular cartilage repair [37].

When placed *in situ*, cartilage scaffolds are exposed to considerable forces acting on the cartilage. When recellularized *in vitro* or *in vivo*, the elastase-treated auricular cartilage scaffolds showed only minor distortion while permitting *in situ* chondrogenic differentiation. This is a considerable benefit because balancing scaffold stiffness – high enough to prevent contraction, but not too high as to repress chondrogenic differentiation – is one of the most challenging aspects of cartilage scaffold design [48]. As expected, the chondrogenic potential of the seeded cells determined glycosaminoglycan restoration and thus compression resistance. We and others have shown that chondrogenic potential of cells varies greatly between donors, age groups and culture protocols [22,49–51]. In earlier studies, we found that WNT signalling agonists prevent the loss of chondrogenic potential during BMSCs expansion, and therefore we expanded all BMSCs with WNT3A [22,52]. Additional methods to improve glycosaminoglycan synthesis, e.g. sorting out the most potent cells, transient genetic manipulation, adjusting culture conditions or providing mechanical stimulation [53–58]

might further enhance restoration of glycosaminoglycan content. Combining these methods with elastase-treated auricular cartilage scaffolds may yield tissue engineered cartilage that approaches the properties of native cartilage. Whether the origin of the chondrogenic cells affects the properties of the generated cartilage, e.g. if nasal septum repair requires nasal chondrocytes, still needs to be explored. The tissue formed by ACs and BMSCs resembled hyaline cartilage, and we have shown earlier that neither auricular nor nasal chondrocytes express elastin *in vitro* [24]. However, auricular chondrocytes form structured elastin fibres in collagen scaffolds when transplanted *in vivo* [59].

A prominent argument for decellularized scaffolds is that the matrix guides cell behaviour in a tissue-specific manner. While the effect on chondrogenic differentiation of aspects such as soluble matrix molecules, structural proteins, glycosaminoglycans, topography and mechanical force transmission have been studied [10,20,60–67], it remains unclear whether cartilage matrix itself stimulates chondrogenesis. Elastase treatment, while chemically mild compared to other decellularization procedures, depletes glycosaminoglycans, thereby likely removing soluble molecules, such as growth factors, bound to them. However, the complex type II collagen network appears to remain intact after elastin removal. Collagen matrices improve chondrogenesis by chondrocytes [68]. Moreover, type II collagen, which is unique to cartilage, has been suggested to increase chondrogenesis in BMSCs [69]. On a larger scale, fibres can guide cell migration and define cell shape [70]. Analysis of the collagen network in elastase-treated auricular cartilage may provide further insight into its role in chondroinduction.

5. Conclusion

Elastase treatment of auricular cartilage provides a scaffold with channels that allow cell migration in the cartilage matrix and guide cells into a distribution resembling that of chondrocytes in native cartilage. When the invading cells, *in vitro* or *in vivo*, restore the glycosaminoglycans lost during elastase treatment, the resulting mixture of native and *de novo* generated matrix partly resembles that of intact articular cartilage. Moreover, the elastase-treated auricular cartilage appears resistant to deformation by cell contraction *in vitro* and *in vivo*, facilitating patient-tailored scaffold design. Our work addresses a major hurdle for cartilage-derived scaffolds: allowing recellularization while keeping the overall cartilage tissue architecture intact. Future research will need to show whether orthotopic zonal structures form upon implantation.

Author Contributions

J.L. conceived the method, designed and ran the experiments, analysed the data and drafted the manuscript. D.t.B, G.J.v.O. and R.N. supervised the project, guided experimental design and manuscript preparation. W.J.L.M.K., N.K. and R.N. assisted with experiment execution. G.J.v.O., S.N., and J.L. developed the concept of the use of elastin channels for auricular cartilage matrix reseeding. S.N. provided feedback on the experimental design. B.C.J.v.d.E. assisted in indentation measurements. K.S. provided feedback on indentation data analysis and experimental set-up.

This research was funded by a bridge grant by the Austrian Research Promotion Agency FFG awarded to S.N. and G.J.v.O. as well as an Erasmus MC grant awarded to G.J.v.O. and D.t.B.

All authors approved the final manuscript.

Acknowledgments

We would like to thank Eric Farrell and colleagues from the Department of Oral & Maxillofacial Surgery at the Erasmus MC for providing paediatric bone marrow-derived mesenchymal stem cells. We would like to thank Cornelia Schneider, Florian Hildner, Susanne Wolbank, Lizette Utomo and Heinz Redl for helpful discussions. The research was financially supported by a bridge grant from Austrian Research Promotion Agency FFG (project Cartiscaff, grant number 842455). J.L., G.J.v.O. and S.N. are listed as inventors on a patent application for the recellularization of cartilage using elastase described in this manuscript. The remaining authors declare no competing financial or other conflicts of interests.

References

[1] A.L. Mescher, L.C.U. Junqueira, Cartilage, in: Junqueira's Basic Histol. Text Atlas, 14th ed., McGraw-Hill Education, 2015: pp. 129–134.

[2] H. Muir, The chondrocyte, architect of cartilage. Biomechanics, structure, function and molecular biology of cartilage matrix macromolecules, BioEssays. 17 (1995) 1039–1048. doi:10.1002/bies.950171208.

[3] J.M. Mansour, Biomechanics of Cartilage, in: Kinesiol. Mech. Pathomechanics Hum. Mov. Second Ed., 2013: pp. 69–83.

[4] A.J. Sophia Fox, A. Bedi, S. a Rodeo, The basic science of articular cartilage: structure, composition, and function., Sports Health. 1 (2009) 461–8. doi:10.1177/1941738109350438.

[5] E.A. Kiyotake, E.C. Beck, M.S. Detamore, Cartilage extracellular matrix as a biomaterial for cartilage regeneration, Ann. N. Y. Acad. Sci. 1383 (2016) 139–159. doi:10.1111/nyas.13278.

[6] C. Schneider, J. Lehmann, G.J.V.M. van Osch, F. Hildner, A. Teuschl, X. Monforte, D. Miosga, P. Heimel, E. Priglinger, H. Redl, S. Wolbank, S. Nürnberger, Systematic Comparison of Protocols for the Preparation of Human Articular Cartilage for Use as Scaffold Material in Cartilage Tissue Engineering, Tissue Eng. Part C Methods. 22 (2016) 1095–1107. doi:10.1089/ten.tec.2016.0380.

[7] K.E.M. Benders, P.R. van Weeren, S.F. Badylak, D.B.F. Saris, W.J.A. Dhert, J. Malda, Extracellular matrix scaffolds for cartilage and bone regeneration, Trends Biotechnol. 31 (2013) 169–176. doi:10.1016/j.tibtech.2012.12.004.

[8] S. Schwarz, L. Koerber, A.F. Elsaesser, E. Goldberg-Bockhorn, A.M. Seitz, L. Dürselen, A. Ignatius, P. Walther, R. Breiter, N. Rotter, Decellularized cartilage matrix as a novel biomatrix for cartilage tissue-engineering applications., Tissue Eng. Part A. 18 (2012) 2195–209. doi:10.1089/ten.TEA.2011.0705.

[9] M. Zang, Q. Zhang, E.I. Chang, A.B. Mathur, P. Yu, Decellularized tracheal matrix scaffold for tracheal tissue engineering: in vivo host response., Plast. Reconstr. Surg. 132 (2013) 549e–559e. doi:10.1097/PRS.0b013e3182a013fc.

[10] E.C. Beck, M. Barragan, T.B. Libeer, S.L. Kieweg, G.L. Converse, R.A. Hopkins, C.J. Berkland, M.S. Detamore, Chondroinduction from Naturally Derived Cartilage Matrix: A Comparison Between Devitalized and Decellularized Cartilage Encapsulated in Hydrogel Pastes, Tissue Eng. Part A. 22 (2016) 665–679. doi:10.1089/ten.tea.2015.0546.

[11] J. Visser, P.A. Levett, N.C.R. te Moller, J. Besems, K.W.M. Boere, M.H.P. van Rijen, J.C. de Grauw, W.J.A. Dhert, P.R. van Weeren, J. Malda, Crosslinkable Hydrogels Derived from Cartilage, Meniscus, and Tendon Tissue, Tissue Eng.

Part A. 21 (2015) 1195–1206. doi:10.1089/ten.tea.2014.0362.

[12] L. Luo, R. Eswaramoorthy, K.J. Mulhall, D.J. Kelly, Decellularization of porcine articular cartilage explants and their subsequent repopulation with human chondroprogenitor cells, J. Mech. Behav. Biomed. Mater. 55 (2016) 21–31. doi:10.1016/j.jmbbm.2015.10.002.

[13] Z. Huang, O. Godkin, G. Schulze-Tanzil, The Challenge in Using Mesenchymal Stromal Cells for Recellularization of Decellularized Cartilage, Stem Cell Rev. Reports. 13 (2017) 50–67. doi:10.1007/s12015-016-9699-8.

[14] K. Willert, J.D. Brown, E. Danenberg, A.W. Duncan, I.L. Weissman, T. Reya, J.R. Yates, R. Nusse, Wnt proteins are lipid-modified and can act as stem cell growth factors, Nature. 423 (2003) 448–452. doi:10.1038/nature01611.

[15] B. Johnstone, T.M. Hering, A.I. Caplan, V.M. Goldberg, J.U. Yoo, In VitroChondrogenesis of Bone Marrow-Derived Mesenchymal Progenitor Cells, Exp. Cell Res. 238 (1998) 265–272. doi:10.1006/excr.1997.3858.

[16] M.L. de Vries-van Melle, E.W. Mandl, N. Kops, W.J.L.M. Koevoet, J.A.N. Verhaar, G.J.V.M. van Osch, An osteochondral culture model to study mechanisms involved in articular cartilage repair, Tissue Eng. Part C Methods. 00 (2011). doi:10.1089/ten.tec.2011.0339.

[17] M.L. de Vries-van Melle, M.S. Tihaya, N. Kops, W.J.L.M. Koevoet, J.M. Murphy, J.A.N. Verhaar, M. Alini, D. Eglin, G.J.V.M. van Osch, Chondrogenic differentiation of human bone marrow-derived mesenchymal stem cells in a simulated osteochondral environment is hydrogel dependent., Eur. Cell. Mater. 27 (2014) 112–23; discussion 123. http://www.ncbi.nlm.nih.gov/pubmed/24488855.

[18] C.A. Schneider, W.S. Rasband, K.W. Eliceiri, NIH Image to ImageJ: 25 years of image analysis., Nat. Methods. 9 (2012) 671–5. doi:22930834.

[19] P.R. Moshtagh, B. Pouran, N.M. Korthagen, A.A. Zadpoor, H. Weinans, Guidelines for an optimized indentation protocol for measurement of cartilage stiffness: The effects of spatial variation and indentation parameters, J. Biomech. 49 (2016) 3602–3607. doi:10.1016/j.jbiomech.2016.09.020.

[20] L. Nimeskern, L. Utomo, I. Lehtoviita, G. Fessel, J.G. Snedeker, G.J.V.M. van Osch, R. Müller, K.S. Stok, Tissue composition regulates distinct viscoelastic responses in auricular and articular cartilage, J. Biomech. 49 (2016) 344–352. doi:10.1016/j.jbiomech.2015.12.032.

[21] H. Nejadnik, J.H. Hui, E.P. Feng Choong, B.-C. Tai, E.H. Lee, Autologous bone marrow-derived mesenchymal stem cells versus autologous chondrocyte implantation: an observational cohort study., Am. J. Sports Med. 38 (2010) 1110–6. doi:10.1177/0363546509359067.

[22] R. Narcisi, M.A. Cleary, P.A.J. Brama, M.J. Hoogduijn, N. Tüysüz, D. ten Berge, G.J.V.M. van Osch, Long-Term Expansion, Enhanced Chondrogenic Potential, and Suppression of Endochondral Ossification of Adult Human MSCs via WNT Signaling Modulation, Stem Cell Reports. (2015). doi:10.1016/j.stemcr.2015.01.017.

[23] R.M. Thiede, Y. Lu, M.D. Markel, A review of the treatment methods for cartilage defects, Vet. Comp. Orthop. Traumatol. 25 (2012) 263–272. doi:10.3415/VCOT-11-05-0070.

[24] C.A. Hellingman, E.T.P. Verwiel, I. Slagt, W. Koevoet, R.M.L. Poublon, G.J. Nolst-Trenité, R.J.B. De Jong, H. Jahr, G.J.V.M. Van Osch, Differences in

Cartilage-Forming Capacity of Expanded Human Chondrocytes from Ear and Nose and Their Gene Expression Profiles, Cell Transplant. 20 (2011) 925–940. doi:10.3727/096368910X539119.

[25] H. Yanaga, K. Imai, T. Fujimoto, K. Yanaga, Generating Ears from Cultured Autologous Auricular Chondrocytes by Using Two-Stage Implantation in Treatment of Microtia, Plast. Reconstr. Surg. 124 (2009) 817–825. doi:10.1097/PRS.0b013e3181b17c0e.

[26] A.L. Ponte, E. Marais, N. Gallay, A. Langonné, B. Delorme, O. Hérault, P. Charbord, J. Domenech, The in vitro migration capacity of human bone marrow mesenchymal stem cells: comparison of chemokine and growth factor chemotactic activities., Stem Cells. 25 (2007) 1737–45. doi:10.1634/stemcells.2007-0054.

[27] Y. Mishima, M. Lotz, Chemotaxis of human articular chondrocytes and mesenchymal stem cells, J. Orthop. Res. 26 (2008) 1407–1412. doi:10.1002/jor.20668.

[28] M.J. Dubon, J. Yu, S. Choi, K.-S. Park, Transforming growth factor β induces bone marrow mesenchymal stem cell migration via noncanonical signals and N-cadherin, J. Cell. Physiol. 233 (2018) 201–213. doi:10.1002/jcp.25863.

[29] N. Shinojima, A. Hossain, T. Takezaki, J. Fueyo, J. Gumin, F. Gao, F. Nwajei, F.C. Marini, M. Andreeff, J.-I. Kuratsu, F.F. Lang, TGF- Mediates Homing of Bone Marrow-Derived Human Mesenchymal Stem Cells to Glioma Stem Cells, Cancer Res. 73 (2013) 2333–2344. doi:10.1158/0008-5472.CAN-12-3086.

[30] A.M. Mackay, S.C. Beck, J.M. Murphy, F.P. Barry, C.O. Chichester, M.F. Pittenger, Chondrogenic Differentiation of Cultured Human Mesenchymal

Stem Cells from Marrow, Tissue Eng. 4 (1998) 415–428. doi:10.1089/ten.1998.4.415.

[31] G.J. van Osch, S.W. van der Veen, P. Buma, H.L. Verwoerd-Verhoef, Effect of transforming growth factor-beta on proteoglycan synthesis by chondrocytes in relation to differentiation stage and the presence of pericellular matrix., Matrix Biol. 17 (1998) 413–24. http://www.ncbi.nlm.nih.gov/pubmed/9840443.

[32] M.R. Homicz, K.B. McGowan, L.M. Lottman, G. Beh, R.L. Sah, D. Watson, A compositional analysis of human nasal septal cartilage., Arch. Facial Plast. Surg. 5 (n.d.) 53–8. http://www.ncbi.nlm.nih.gov/pubmed/12533140.

[33] R.A. Stockwell, The cell density of human articular and costal cartilage., J. Anat. 101 (1967) 753–63. http://www.ncbi.nlm.nih.gov/pubmed/6059823.

[34] C.R. Lee, H.A. Breinan, S. Nehrer, M. Spector, Articular cartilage chondrocytes in type I and type II collagen-GAG matrices exhibit contractile behavior in vitro., Tissue Eng. 6 (2000) 555–65. doi:10.1089/107632700750022198.

[35] L. Zhou, I. Pomerantseva, E.K. Bassett, C.M. Bowley, X. Zhao, D.A. Bichara, K.M. Kulig, J.P. Vacanti, M.A. Randolph, C.A. Sundback, Engineering Ear Constructs with a Composite Scaffold to Maintain Dimensions, Tissue Eng. Part A. 17 (2011) 1573–1581. doi:10.1089/ten.tea.2010.0627.

[36] S. Röker, S. Diederichs, Y. Stark, S. Böhm, I. Ochoa, J.A. Sanz, J.M. García-Aznar, M. Doblaré, M. van Griensven, T. Scheper, C. Kasper, Novel 3D biomaterials for tissue engineering based on collagen and macroporous ceramics, Materwiss. Werksttech. 40 (2009) 54–60. doi:10.1002/mawe.200800413.

[37] R.M. Thiede, Y. Lu, M.D. Markel, A review of the treatment methods for cartilage defects., Vet. Comp. Orthop. Traumatol. 25 (2012) 263–72. doi:10.3415/VCOT-11-05-0070.

[38] A. Lolli, R. Narcisi, E. Lambertini, L. Penolazzi, M. Angelozzi, N. Kops, S. Gasparini, G.J.V.M. van Osch, R. Piva, Silencing of Antichondrogenic MicroRNA-221 in Human Mesenchymal Stem Cells Promotes Cartilage Repair In Vivo, Stem Cells. 34 (2016) 1801–1811. doi:10.1002/stem.2350.

[39] C.A. Bautista, H.J. Park, C.M. Mazur, R.K. Aaron, B. Bilgen, Effects of Chondroitinase ABC-Mediated Proteoglycan Digestion on Decellularization and Recellularization of Articular Cartilage, PLoS One. 11 (2016) e0158976. doi:10.1371/journal.pone.0158976.

[40] D.E.T. Shepherd, B.B. Seedhom, Thickness of human articular cartilage in joints of the lower limb, Ann. Rheum. Dis. 58 (1999) 27–34. doi:10.1136/ard.58.1.27.

[41] K. Hwang, F. Huan, D.J. Kim, Mapping Thickness of Nasal Septal Cartilage, J. Craniofac. Surg. 21 (2010) 243–244. doi:10.1097/SCS.0b013e3181c5a203.

[42] K.R. Stone, A.W. Walgenbach, J.T. Abrams, J. Nelson, N. Gillett, U. Galili, Porcine and bovine cartilage transplants in cynomolgus monkey: I. A model for chronic xenograft rejection., Transplantation. 63 (1997) 640–5. http://www.ncbi.nlm.nih.gov/pubmed/9075831 (accessed January 27, 2014).

[43] J. Gille, P. Behrens, A.P. Schulz, R. Oheim, B. Kienast, Matrix-Associated Autologous Chondrocyte Implantation, Cartilage. 7 (2016) 309–315. doi:10.1177/1947603516638901.

[44] R.A. Manji, W. Lee, D.K.C. Cooper, Xenograft bioprosthetic heart valves: Past, present and future, Int. J. Surg. 23 (2015) 280–284. doi:10.1016/j.ijsu.2015.07.009.

[45] P.K. Bos, M. van Melle, G.J.V.M. van Osch, Articular cartilage repair and the evolving role of regenerative medicine, Open Access Surg. (2010) 109. doi:10.2147/OAS.S7192.

[46] M. Mumme, A. Barbero, S. Miot, A. Wixmerten, S. Feliciano, F. Wolf, A.M. Asnaghi, D. Baumhoer, O. Bieri, M. Kretzschmar, G. Pagenstert, M. Haug, D.J. Schaefer, I. Martin, M. Jakob, Nasal chondrocyte-based engineered autologous cartilage tissue for repair of articular cartilage defects: an observational first-in-human trial, Lancet. 388 (2016) 1985–1994. doi:10.1016/S0140-6736(16)31658-0.

[47] N.C. Hidvegi, K.M. Sales, D. Izadi, J. Ong, P. Kellam, D. Eastwood, P.E.M. Butler, A low temperature method of isolating normal human articular chondrocytes, Osteoarthr. Cartil. 14 (2006) 89–93. doi:10.1016/j.joca.2005.08.007.

[48] A.J. Steward, D.J. Kelly, Mechanical regulation of mesenchymal stem cell differentiation, J. Anat. 227 (2015) 717–731. doi:10.1111/joa.12243.

[49] S. Yanada, M. Ochi, K. Kojima, P. Sharman, Y. Yasunaga, E. Hiyama, Possibility of selection of chondrogenic progenitor cells by telomere length in FGF-2-expanded mesenchymal stromal cells., Cell Prolif. 39 (2006) 575–84. doi:10.1111/j.1365-2184.2006.00397.x.

[50] N. Baker, L.B. Boyette, R.S. Tuan, Characterization of bone marrow-derived mesenchymal stem cells in aging, Bone. 70 (2015) 37–47.

doi:10.1016/j.bone.2014.10.014.

[51] C.A. Knuth, C.H. Kiernan, V. Palomares Cabeza, J. Lehmann, J. Witte-Buoma, D. ten Berge, P.A.J. Brama, E.B. Wolvius, E.M. Strabbing, M. Koudstaal, R. Narcisi, E. Farrell, Isolating paediatric mesenchymal stem cells with enhanced expansion and differentiation capabilities, Tissue Eng. Part C Methods. (2018) ten.TEC.2018.0031. doi:10.1089/ten.TEC.2018.0031.

[52] R. Narcisi, O.H. Arikan, J. Lehmann, D. ten Berge, G.J.V.M. van Osch, Differential Effects of Small Molecule WNT Agonists on the Multilineage Differentiation Capacity of Human Mesenchymal Stem Cells, Tissue Eng. Part A. 22 (2016) 1264–1273. doi:10.1089/ten.tea.2016.0081.

[53] M.K. Majumdar, E. Wang, E. a Morris, BMP-2 and BMP-9 promotes chondrogenic differentiation of human multipotential mesenchymal cells and overcomes the inhibitory effect of IL-1., J. Cell. Physiol. 189 (2001) 275–84. doi:10.1002/jcp.10025.

[54] C.C. Tsai, Y.J. Chen, T.L. Yew, L.L. Chen, J.Y. Wang, C.H. Chiu, S.C. Hung, Hypoxia inhibits senescence and maintains mesenchymal stem cell properties through down-regulation of E2A-p21 by HIF-TWIST, Blood. 117 (2011) 459–469. doi:10.1182/blood-2010-05-287508.

[55] E.A. Makris, D.J. Responte, N.K. Paschos, J.C. Hu, K.A. Athanasiou, Developing functional musculoskeletal tissues through hypoxia and lysyl oxidase-induced collagen cross-linking, Proc. Natl. Acad. Sci. 111 (2014) E4832–E4841. doi:10.1073/pnas.1414271111.

[56] A. Lolli, E. Lambertini, L. Penolazzi, M. Angelozzi, C. Morganti, T. Franceschetti, S. Pelucchi, R. Gambari, R. Piva, Pro-chondrogenic effect of

miR-221 and slug depletion in human MSCs., Stem Cell Rev. 10 (2014) 841–55. doi:10.1007/s12015-014-9532-1.

[57] K. Sivasubramaniyan, A. Harichandan, P. Boss, H.-J. Buehring, G. van Osch, Isolation of phenotypically and functionally distinct endogeneous human bone marrow-derived mesenchymal stem/stromal cell subsets, Osteoarthr. Cartil. 24 (2016) S464. doi:10.1016/j.joca.2016.01.846.

[58] D. Schumann, R. Kujat, M. Nerlich, P. Angele, Mechanobiological conditioning of stem cells for cartilage tissue engineering., Biomed. Mater. Eng. 16 (2006) S37-52. http://www.ncbi.nlm.nih.gov/pubmed/16823112.

[59] X. Zhao, D.A. Bichara, L. Zhou, K.M. Kulig, A. Tseng, C.M. Bowley, J.P. Vacanti, I. Pomerantseva, C.A. Sundback, M.A. Randolph, Conditions for seeding and promoting neo-auricular cartilage formation in a fibrous collagen scaffold, J. Cranio-Maxillofacial Surg. 43 (2015) 382–389. doi:10.1016/j.jcms.2014.12.007.

[60] A.J. Sutherland, E.C. Beck, S.C. Dennis, G.L. Converse, R.A. Hopkins, C.J. Berkland, M.S. Detamore, Decellularized Cartilage May Be a Chondroinductive Material for Osteochondral Tissue Engineering, PLoS One. 10 (2015) e0121966. doi:10.1371/journal.pone.0121966.

[61] V. Gupta, K.M. Tenny, M. Barragan, C.J. Berkland, M.S. Detamore, Microsphere-based scaffolds encapsulating chondroitin sulfate or decellularized cartilage, J. Biomater. Appl. 31 (2016) 328–343. doi:10.1177/0885328216655469.

[62] B.O. Diekman, C.R. Rowland, D.P. Lennon, A.I. Caplan, F. Guilak, Chondrogenesis of adult stem cells from adipose tissue and bone marrow:

induction by growth factors and cartilage-derived matrix., Tissue Eng. Part A. 16 (2010) 523–33. doi:10.1089/ten.TEA.2009.0398.

[63] N.W. Garrigues, D. Little, J. Sanchez-Adams, D.S. Ruch, F. Guilak, Electrospun cartilage-derived matrix scaffolds for cartilage tissue engineering, J. Biomed. Mater. Res. Part A. 102 (2014) 3998–4008. doi:10.1002/jbm.a.35068.

[64] N.-C. Cheng, B.T. Estes, H.A. Awad, F. Guilak, Chondrogenic Differentiation of Adipose-Derived Adult Stem Cells by a Porous Scaffold Derived from Native Articular Cartilage Extracellular Matrix, Tissue Eng. Part A. 15 (2009) 231–241. doi:10.1089/ten.tea.2008.0253.

[65] Y.Y. Gong, J.X. Xue, W.J. Zhang, G.D. Zhou, W. Liu, Y. Cao, A sandwich model for engineering cartilage with acellular cartilage sheets and chondrocytes, Biomaterials. 32 (2011) 2265–2273. doi:10.1016/j.biomaterials.2010.11.078.

[66] G.C. Ingavle, A.W. Frei, S.H. Gehrke, M.S. Detamore, Incorporation of Aggrecan in Interpenetrating Network Hydrogels to Improve Cellular Performance for Cartilage Tissue Engineering, Tissue Eng. Part A. 19 (2013) 1349–1359. doi:10.1089/ten.tea.2012.0160.

[67] Y. Zhang, S. Chen, M. Pei, Biomechanical signals guiding stem cell cartilage engineering: from molecular adaption to tissue functionality., Eur. Cell. Mater. 31 (2016) 59–78. http://www.ncbi.nlm.nih.gov/pubmed/26728499.

[68] M.H. Cha, S.H. Do, G.R. Park, P. Du, K.-C. Han, D.K. Han, K. Park, Induction of Re-Differentiation of Passaged Rat Chondrocytes Using a Naturally Obtained Extracellular Matrix Microenvironment, Tissue Eng. Part A. 19 (2013)

978–988. doi:10.1089/ten.tea.2012.0358.

[69] Y.-N. Wu, Z. Yang, J.H.P. Hui, H.-W. Ouyang, E.H. Lee, Cartilaginous ECM component-modification of the micro-bead culture system for chondrogenic differentiation of mesenchymal stem cells, Biomaterials. 28 (2007) 4056–4067. doi:10.1016/j.biomaterials.2007.05.039.

[70] M.P. Lutolf, J.A. Hubbell, Synthetic biomaterials as instructive extracellular microenvironments for morphogenesis in tissue engineering, Nat. Biotechnol. 23 (2005) 47–55. doi:10.1038/nbt1055.

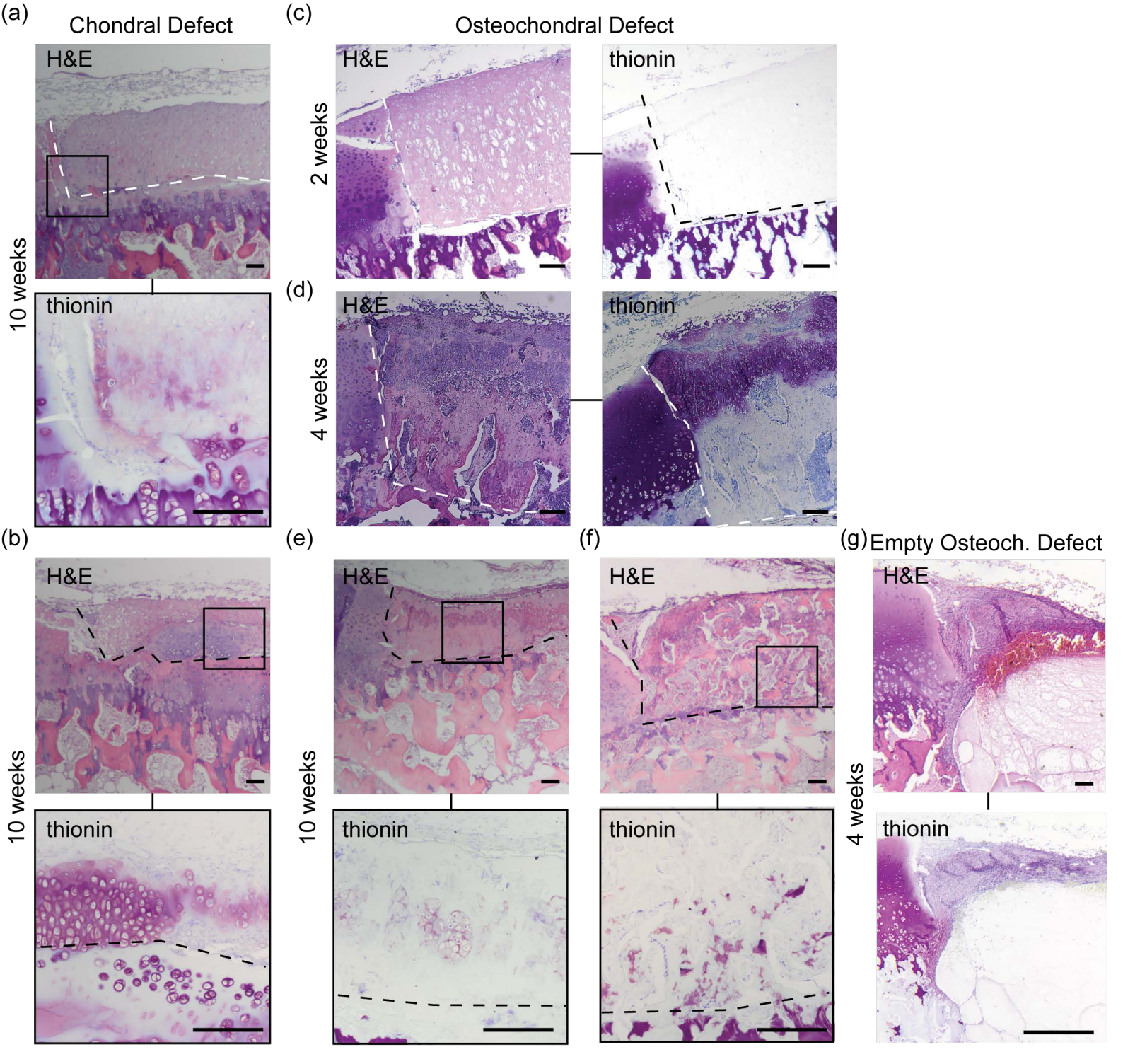
(a)
Chondral Defect
H&E
10 weeks
thionin
(c)
Osteochondral Defect
H&E
thionin
2 weeks
(d)
H&E
thionin
4 weeks
(b)
H&E
10 weeks
thionin
(e)
H&E
10 weeks
thionin
(f)
H&E
thionin
(g)
Empty Osteoch. Defect
H&E
4 weeks
thionin